

# Quantifying biological effects of radiation from high-energy linear accelerators on lymphocytes

Gyöngyi Farkas<sup>1</sup>, Zsuzsa S. Kocsis<sup>1</sup>, Gábor Székely<sup>1</sup>, Dalma Mihály<sup>2</sup>,  
Csilla Pesznyák<sup>3</sup>, Tamás Pócza<sup>2</sup>, Tibor Major<sup>2</sup>, Csaba Polgár<sup>4</sup> and Zsolt Jurányi<sup>1,\*</sup>

<sup>1</sup>National Institute of Oncology, Centre of Radiotherapy, Department of Radiobiology and Diagnostic Onco-Cytogenetics, 1122 Budapest, Ráth György u.7-9

<sup>2</sup>National Institute of Oncology, Centre of Radiotherapy, 1122 Budapest, Ráth György u.7-9

<sup>3</sup>Budapest University of Technological Economics Hungary, National Institute of Oncology, Centre of Radiotherapy, 1122 Budapest, Ráth György u.7-9

<sup>4</sup>Centre of Radiotherapy, National Institute of Oncology, Budapest, Hungary, Department of Oncology, Semmelweis University, Budapest, Hungary, 1122 Budapest, Ráth György u.7-9

\*Corresponding author. National Institute of Oncology, Centre of Radiotherapy, Department of Radiobiology and Diagnostic Onco-Cytogenetics, 1122 Budapest, Ráth György u.7-9. Tel: 36 1-224 8779; Email: juranyi.zsolt@oncol.hu

(Received 9 May 2019; revised 23 July 2019; editorial decision 26 September 2019)

## ABSTRACT

The aim of this study was to investigate the radiobiological effects of flattening filter (FF) and flattening filter-free (FFF) modes of linear electron accelerators and to understand whether there is any difference between the effects of these modes. We evaluated the number of chromosome aberrations following irradiation of lymphocytes from healthy volunteers with X-ray photons at two energy levels, 6 and 10 MV; the dose rate ranged between 5.50 and 23.08 Gy/min and absorbed doses ranged between 0.5 and 8 Gy. A <sup>60</sup>Co curve was employed for comparison. Metaphases from the lymphocyte cultures were prepared using standard cytogenetic techniques and chromosome analysis was performed. Our results allow the performance of biodosimetry at higher energies and doses than the currently used reference dosimetry. We observed significant differences in aberration frequencies when different irradiation techniques were used. FFF mode has a higher radiobiological effect than the FF mode. Linear-quadratic dose response calibration curves were constructed and relative biological effectiveness (RBE) values were calculated. Average RBE values using 6 MV (5.50 Gy/min) as a reference radiation were 1.28 for <sup>60</sup>Co  $\gamma$  irradiation, 1.11 for 6 FFF and 0.79–0.92 for 10 FFF. Since there are compelling differences between radiation modalities in cases of hypofractionation, these results may be even more important in a therapeutic situation. In case of an accidental overdose of a patient, use of the appropriate calibration curves for biodosimetry are also essential for quantifying the overdose.

**Keywords:** biological dosimetry; flattening filter-free mode; linear accelerator; dicentric chromosome

## INTRODUCTION

Biological dosimetry has an important role in the investigation of radiation accidents, and it can provide useful information on therapeutic techniques as well [1].

A number of papers have presented dose–response curves for dicentric plus rings induced by 250 kVp X-rays, <sup>137</sup>Cs and <sup>60</sup>Cobalt gamma rays [2, 3]. However, in the past few years many <sup>60</sup>Co (1.25 MV) sources have been replaced by electron linear accelerators (LINACs), increasing the need for new biodosimetry calibration curves most suitable for energy levels >4 MV in order to be prepared for dosimetric accidents [4–6].

The effect of ionizing radiation in biological systems depends not only on the applied dose, but also on the energy and such parameters as

dose rates and filters [7]. The same electron beam with equal nominal energy is used to create both flattening filter (FF) and flattening filter-free (FFF) photon beams. Therefore, electron energy at the target is the same in both cases and the removal of the FF increases output, but also reduces the penetrative quality of the photon beam due to reduced beam hardening. The FFF beams have a different beam profile and photon energy spectrum. The FFF mode also increases beam intensity and reduces treatment time, especially for high-dose stereotactic radiotherapy/radiosurgery.

There is a scarcity of information about the high dose range, although Vinnikov *et al.* and Pujol *et al.* [8–10] provided some experimental data on the radiobiological effect of high doses (5–20 Gy). This dose range is particularly important for handling cases

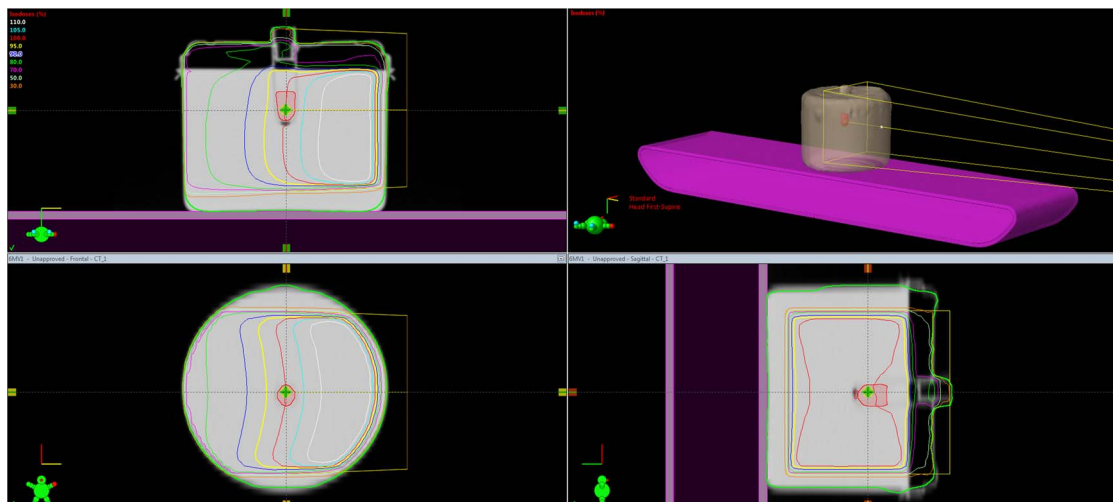


Fig. 1. Treatment plan of the irradiation. CT scan of the plastic phantom with the cryotube in the central axis.

**Table 1. The applied energy and nominal dose rates of the linear accelerator and the actual dose rates in the blood samples**

Energy	Nominal MU/min	Actual Gy/min
6 MV	600	5.50
10 MV	600	5.88
6 FFF	600	5.36
6 FFF	1400	12.5
10 FFF	400	3.85
10 FFF	1600	15.40
10 FFF	2400	23.08

of health- or life-threatening radiation exposures. Extending the range of radiation qualities for which the dicentric assay has been calibrated is also highly necessary because of advances in medical treatment techniques with LINACs. However, in most of these experiments donors' blood was irradiated with a cobalt (gamma) source and the dose rate was between 0.5 Gy/min and 1.2 Gy/min.

The high dose rates of an FFF beam have re-introduced discussions about the radiobiological consequences of high dose rates for both normal tissues and tumors [11]. For example Lohse *et al.* examined the radiobiological effect of the FF and FFF beams using two glioblastoma cell lines, which were irradiated with either 5 or 10 Gy using different dose rates [12]. Dose verification was performed and colony formation assays were carried out. The results demonstrated that irradiation of glioblastoma cell lines using the FFF beam is more efficient in reducing clonogenic cell survival than the standard flattened beam. In contrast, according to Verbakel *et al.* FFF irradiation with a dose rate of 2400 MU/min did not change cell survival for three human cancer cell lines up to a fraction dose of 12 Gy compared with irradiation using FF beams [13]. In summary, these rare and controversial studies used colony formation assays, and data in the case of normal, non-cancerous cells are still missing.

We used peripheral blood lymphocytes, because they circulate throughout the body and are a good model for biodosimetric assays [14, 15]. We investigated the cytogenetic effect of different techniques at the level of all chromosomal aberration types and determined which aberration is suitable for biological dosimetry besides dicentric plus rings in these cases. Our goal was to identify the potential and substantial differences in cytogenetic parameters in clinical settings that can have important therapeutic effects, especially for hypofractionated schedules. The results obtained were compared with curves found in published studies in which various types of radiation were used to investigate differences in the linear and quadratic terms for different radiation energies.

## MATERIALS AND METHODS

This study was approved by the Hungarian Ethical Committee, ETT TUKEB (23546-3/201) (23546-3/2017/EKU) and was conducted following the principles of the Helsinki Declaration. All subjects were informed about the aim of the study and gave their written consent.

### Irradiation of blood samples

Blood samples in 2 mL cryotubes were irradiated in a water-filled plastic phantom (the bottom of the cryotube was 4 cm below the surface of the water) at room temperature in order to achieve homogenous doses. A TrueBeam linear accelerator (Varian, Palo Alto, USA) was used for irradiation with an Eclipse 13.6 treatment planning system. The machine was calibrated in water according to the IAEA TRS-398 protocol. 1 MU corresponds to 1 cGy at dose maximum, with 100 cm source surface distance (SSD). The absolute calibration was performed with a PTW 30010 Farmer chamber (Freiburg, Germany). The samples were positioned at the isocenter (Fig. 1) with 95 cm SSD. The gantry angle was 90 degrees and the field size was  $8 \times 8$  cm at the isocenter. Table 1. shows the different dose rates expressed as Gy/min. These are the only available dose rates, for our measurements these settings were used. These dose

rates are preprogrammed values of the linear accelerator therefore these settings were used in our experiments. The doses ranged from 0.5 to 8 Gy.

### Lymphocyte cultures

For preparation of the dose rate curves, venous blood samples were obtained by venipuncture from 19 healthy non-smoker volunteers (age:  $38.5 \pm 11.2$  years, female: 11, male: 8) and were placed into Li-heparinised vacutainers. To validate the dose–response curves, blood samples were taken from five patients (age:  $70 \pm 5.5$  years, female: 1, male: 4) and were irradiated with 3 and 6 Gy (6 FFF, 12.5 Gy/min). The lymphocytes were cultured using standard cytogenetic techniques immediately after the exposure: 0.8 mL of blood was added to 9 mL of RPMI-1640 cell culture medium containing 15% bovine serum albumin and penicillin/streptomycin (0.5 mL/L). Lymphocyte proliferation was induced with phytohaemagglutinin M (0.2%). The samples were incubated for 52 h at 37°C. Cell proliferation was inhibited with 0.1 µg/ml Colcemid (Gibco) in the last 2 h of culturing. Cell cultures were then centrifuged, hypotonized with 0.075 M KCl for 15 min at 37°C and fixed with cold methanol–acetic acid 3:1 mixture. Following several washes in fresh fixative, the cells were gathered in a small volume of fresh fixative, and this suspension was dropped on glass slides, dried and stained with 3% Giemsa.

### Study of chromosomal aberrations

More than 200 metaphases were analyzed per each experimental point using a light microscope (Olympus BX51 with 100x Plan apo oil immersion objective and 15x eyepiece). Chromosome analysis was performed at the first cell division. Only clear oval metaphase cells were counted. Based on the structural differences, chromatid-type breaks (chromatid break, exchange) and chromosomal-type breaks and rearrangements (fragments, dicentrics, rings, translocations) were identified. One dicentric or ring and one acentric fragment observed in the examined cell were counted together as one chromosome aberration (CA). Excess fragments were not distinguished as terminal or interstitial deletions according to the position of the chromatin loss. Acentric fragments not associated with dicentric or ring aberrations were counted as excess fragments. One trivalent chromosome was counted as two dicentric equivalents. The evaluation was made in accordance with the requirements of ICPENC [16]. The slides were coded and metaphases were analysed by four experienced investigators. Each one scored a subset of the slides to lessen the bias from individual scorers and different slides.

### Statistical analysis

The yields of aberrant cells and aberrations (Y) were expressed per 100 cells scored. Standard errors (SE) of the mean of the aberration yield were calculated from the dispersion ( $\sigma^2$ ) of aberration among cell distributions. At each experimental point aberrations among cell distributions were checked for consistency with a Poisson model using the variance to mean ratio ( $\sigma^2/Y$ ) and Papworth's u-test [17]. Fitting the dose response to the linear-quadratic model was carried out by the iteratively reweighted least-squares method. Student's t-test was used for statistical analyzes. Significant differences were determined

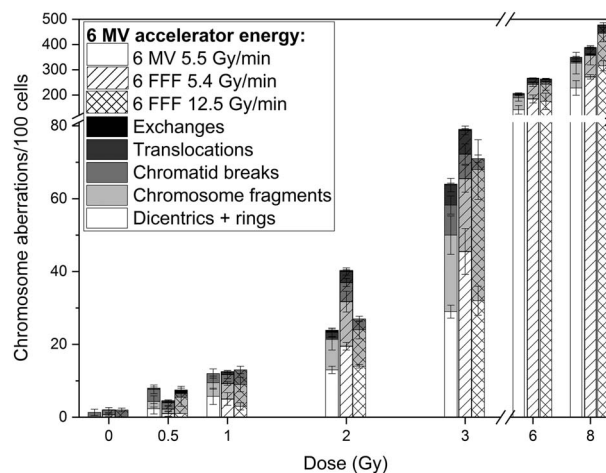


**Fig. 2.** Frequencies of dicentrics + rings, chromosome fragments, translocations, total aberrations in human blood lymphocytes of two donors irradiated by 6 MV/FFF photon beam at different dose rates.

with 95% confidence interval,  $P$  value of  $< 0.05$  was considered as the limit of significance. Dose–response was fitted using CABAS-2 (Chromosomal Aberration Calculation) software [18]. GraphPad InStat 3, GraphPad Prism 5 and Origin Pro 9 software packages were used for calculations and data presentation [19].

## RESULTS

### Comparing the biological effects of different modalities in chromosome aberrations measured at 6–10 MV photon energy with or without FF

Each donor's blood sample was irradiated with dose rates ranging from 3.85–to 23.08 Gy/min (Table 1) and energy between 6–10 MV with a dose of 0.5–8 Gy. All dose–response curves were calculated from the blood samples of four different individuals. One non-irradiated aliquot served as a control sample on every occasion. (To eliminate the effect of individual sensitivity the same donor's blood sample was irradiated for the comparison of 6 MV in FFF and FF mode). For scoring, 100–200 complete metaphase cells were counted (blindly) per dose point per donor under every condition.

We observed significant differences between the frequencies of dicentrics plus rings at absorbed dose ranging between 2 and 8 Gy 6 MV FF 5.50 Gy/min vs 6 MV FFF 5.36 Gy/min ( $P < 0.0001$ ); 6 MV FF 5.50 Gy/min vs 6 MV FFF 5.36 Gy/min ( $P = 0.013$ ); 6 MV FF 5.50 Gy/min vs 6 MV FFF 5.36 Gy/min ( $P < 0.001$ ) and 6 MV FF 5.50 Gy/min vs 6 MV FFF 12.50 Gy/min ( $P < 0.001$ ). There were also significant differences in the number of total aberrations at 2 and 8 Gy (Fig. 2).

The effects of conventional irradiation techniques (chromosomal aberrations) were also compared for the same donor's blood samples using 10 MV FF and FFF modes and dose rates with the 5.88 Gy/min 10 MV FF mode and 3.85, 15.40 and 23.08 Gy/min (Fig. 3). The aberration frequencies (dicentrics + rings) were significantly higher

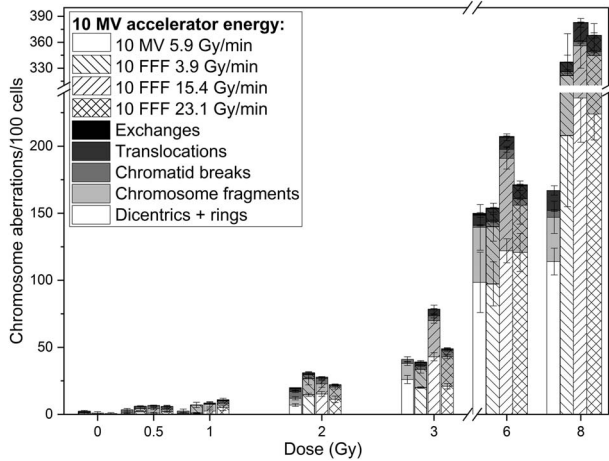


**Fig. 3.** Frequencies of dicentrics + rings, chromosome fragments, translocations, total aberrations, in human blood lymphocytes of two donors irradiated by 10 MV/FFF photon beam at different dose rates.

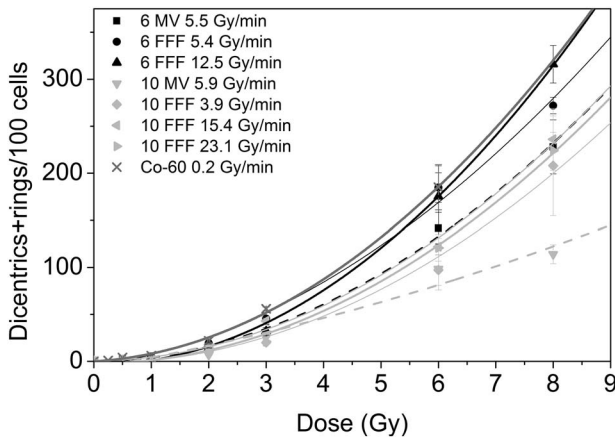


**Fig. 4.** Dose–response calibration curves for dicentrics + rings induced by irradiation with LINAC X-rays. Fitted linear quadratic model curves are represented by lines.

$Y = c + \alpha D + \beta D^2$ , where  $Y$  is the number of dicentric and ring chromosomes/number of metaphase spreads scored,  $D$  is radiation dose,  $c$  is background level, and  $\alpha$  is the linear and  $\beta$  is the quadratic coefficient. Vertical bars indicate standard errors of the observed yields. Calibration curve of 6 FFF at 12.5 Gy/min:  $Y = (0.001 \pm 0.001) + (0.012 \pm 0.011)D + (0.046 \pm 0.002)D^2$ .

between 2 and 8 Gy ( $P < 0.05$ ) at 10 MV FFF 3.85, 15.40 and 23.08 Gy/min than at 10 MV FF 5.88 Gy/min, the differences in total aberrations were significant between 3 and 8 Gy ( $P < 0.0001$ ). Dicentrics plus rings and total aberrations were significantly higher at 6 MV FFF mode than at 10 MV FFF mode for 2 ( $P = 0.001$ ) and 8 ( $P = 0.011$ ) Gy (Fig. 2 and 3).

### Relation to other chromosome- and chromatid-type aberrations

We could not find significant differences in frequencies of chromatid breaks, exchanges (both chromatid-type aberrations), chromosome fragments (excess fragments) and translocations (Fig. 2 and Fig. 3) (chromosome-type aberrations) at different energies or at FF vs FFF mode. In 6 MV FFF 5.36 Gy/min at 0.5 Gy, dicentrics plus rings represented 22.2% of the total aberrations and at 8 Gy this value was 70.1%, while at 10 MV FFF 3.85 Gy/min these values were 33.3% (at 0.5 Gy) and 61.7% (at 8 Gy), respectively. The ratio of the yields of dicentrics to centric rings was  $\sim 5$ – $10$ :1 and was independent of the dose. Dicentrics were about as common as excess fragments at  $\leq 2$  Gy, and were  $\sim$ two times more frequent than excess fragments at  $\geq 3$  Gy.

At lower doses (0.5–1 Gy), chromatid breaks and acentrics (not to be confused with the dicentric or ring coupled fragments) exceeded the number of dicentrics plus rings, however, at higher doses ( $> 2$  Gy) this tendency was reversed, and the dicentrics plus rings predominated.

Excess fragments are 40.5–60.4% of dicentrics at 8 Gy and the ratio depends on energy. The rate of translocations, which can still be scored with conventional Giemsa staining, is ten times less than that of dicentrics plus rings (range: 0–38/100 cells) and their frequencies also grew quadratically with the dose. As Giemsa-stained translocations are not always distinguishable (in 10% of the translocations) our method is not directly comparable with translocation results using Fluorescence in situ hybridization (FISH) methodology. On the other hand, more metaphases can be analysed with the Giemsa method. In our work, the number of chromatid breaks increased with the dose linearly and the maximum value was 14/100 cells at 6 Gy. There is no significant difference between frequencies of chromatid breaks among the irradiation techniques used. However, chromatid breaks are not specific and are less significant for irradiation.

The other chromatid-type aberrations investigated were the exchanges, they were less frequent than chromatid breaks. The highest yield of exchanges at 6 FFF was 3/100 cells.

### Formal fitting of dose–response data to the linear-quadratic model

The background level of chromosome aberration is very important for dose estimation assessment. For the dicentric technique, we obtained data from 19 healthy people. The average background level was 6 dicentrics plus rings in 6000 cells (0.001 dicentrics plus rings/cells). This value coincides with the results of our previous population survey [20]. After *in vitro* irradiation with either 6 or 10 MV FF and FFF modes, a total of 28 000 metaphase spreads were counted, and all stable and unstable chromosomal aberrations were recorded. The distributions of dicentrics plus rings were in accordance with the Poisson model (average  $U$  value was 0.119). Fig. 4 shows the dose–response calibration curves for dicentrics plus rings induced by irradiation with LINAC X-rays. Data are fitted with CABAS. Factors like the energies employed and the dose rate directly influenced the values of  $\beta$ . At 6 MV FF and FFF mode the values of  $\beta$  (0.037 and 0.045  $\text{Gy}^{-2}$  respectively) were higher than at 10 MV FF and FFF mode (0.023 and 0.036  $\text{Gy}^{-2}$ , respectively). The



**Table 2.** Comparison of linear and quadratic yield coefficients and goodness of fit parameters calculated with CABAS software (data of one person).  $\alpha$  and  $\beta$  values are the coefficients of linear and quadratic terms; SE = standard error, DF = degrees of freedom, P = probability for four degrees of freedom at 5 percent.

Energy, MV dose rate, Gy/min	$\alpha$ value $\pm$ SE, Gy <sup>-1</sup>	$\beta$ value $\pm$ SE, Gy <sup>-2</sup>	Chi <sup>2</sup>	DF	P <sup>5%</sup>
6 FFF 12.50	0.012 $\pm$ 0.011	0.046 $\pm$ 0.002	4.93	4	9.48
6 FFF 5.36	0.007 $\pm$ 0.006	0.044 $\pm$ 0.001	17.51	4	9.48
6 MV 5.50	0.020 $\pm$ 0.008	0.033 $\pm$ 0.002	3.65	4	9.48
10 MV 5.88	0.0009 $\pm$ 0.008	0.023 $\pm$ 0.002	17.20	4	9.48
10 FFF 3.85	0.004 $\pm$ 0.008	0.025 $\pm$ 0.002	4.46	4	9.48
10 FFF 15.40	0.013 $\pm$ 0.011	0.033 $\pm$ 0.002	10.89	4	9.48
10 FFF 23.08	0.007 $\pm$ 0.012	0.030 $\pm$ 0.002	9.89	4	9.49

**Table 3.**  $\alpha$  and  $\beta$  values of the dose rate curves; every value is an average of 2–6 dose rate curves.

Energy, MV	Dose rate, Gy/min	$\alpha$ value, Gy <sup>-1</sup>	$\beta$ value, Gy <sup>-2</sup>
6 FFF	12.50	0.006 $\pm$ 0.005	0.045 $\pm$ 0.002
6 FFF	5.36	0.008 $\pm$ 0.001	0.044 $\pm$ 0.0007
6 MV	5.50	0.002 $\pm$ 0.001	0.037 $\pm$ 0.005
10 FFF	23.08	0.007 $\pm$ 0.002	0.036 $\pm$ 0.003
10 FFF	15.40	0.001 $\pm$ 0.007	0.036 $\pm$ 0.002
10 FFF	3.85	0.009 $\pm$ 0.010	0.027 $\pm$ 0.001
10 MV	5.88	0.0009 $\pm$ 0.0008	0.029 $\pm$ 0.007

$\beta$  values were the highest (0.044  $\pm$  0.001 Gy<sup>-2</sup>) at 6 FFF mode (with 12.5 Gy/min), the lowest  $\beta$  values were (0.023  $\pm$  0.002 Gy<sup>-2</sup>) at 10 MV FF (with 5.88 Gy/min). The values of  $\alpha$  component were lower than  $\beta$  values, and the lowest and highest values were: 0.0009 and 0.020 Gy<sup>-1</sup>, respectively (Tables 2 and 3). Linear coefficients decreased with increasing photon energy. We also employed dose estimation calculations based on all of the measured curves and found correspondence with the dose range of the measured data. There is an  $\sim$ 0.2 Gy difference between steeper and flatter curves at 0.5 Gy, but this value can be 1 Gy in the 6–7 Gy dose range. Generally, the degree of variability in the predicted dose is greater at higher doses than in lower doses. If only the 0–3 Gy dose range was included in our calculations, then we would receive higher  $\alpha$  and lower  $\beta$  values than in the 0–8 Gy dose range. The linear coefficients tend to be reduced at higher energies. There are also expected differences between the dose rate curves we have recorded: the yield of dicentric plus rings increased with the radiation dose, showing increments that were clearly dose-dependent.

We compared our results with data retrieved from the literature [21, 22]. Wilkins *et al.* and Prasanna *et al.* published tables for comparison of results between laboratories. We also used the estimated doses for comparison, but extended the tables with the data of 100 and 200 dicentrics. We also calculated the doses for the other mentioned publications and our data, applying CABAS software (Table 4). These comparisons demonstrated that there were no significant differences between our and other authors' dose rate curves at 2 dicentrics plus rings/100 cells frequency at different applied energies (Table 4). However, in the case of 20–200 dicentrics plus rings/100 cells, there are significant differences. For example, at 20 dicentrics plus rings/100

cells, there is a significant change between the estimated dose of 6 MV FF 0.54 Gy/min [4] and 10 MV FF 5.58 Gy/min (our data). There were significant differences between the calculated estimated doses obtained in our experiments and those of Lemos-Pinto *et al.* [4] (at 6 and 10 MV energies with FF and FFF modes). Using our own dose rate curves (6 MV FFF and 10 MV FFF) we estimated higher doses than other authors [2, 8, 21, 23] with cobalt gamma sources or 6 MV LINAC [4]. These calculations are important during hypofractionated radiotherapy because we can influence the biological effect of treatment with energy and dose rate of irradiation. For example, 200 dicentric plus ring aberrations/100 cells predicts a 6.7 Gy dose at 6 MV FFF (12.5 Gy/min) or 8.0 Gy dose at 10 MV FFF (23.08 Gy/min). That is, the 6 FFF, 12.5 Gy/min has a greater biological effect than the 10 FFF, 23.08 Gy/min.

To compare the effect of the different photon energies and dose rates used, relative biological effectiveness (RBE) values were calculated based on the dose–response results obtained. RBE is defined as the ratio of the dose given by a reference radiation quality and the dose given by a test radiation that produce equal effect. We used 6 MV FF (5.50 Gy/min) as the reference radiation. The average RBE value was 1.11 for 6 MV FFF (5.36–12.50 Gy/min), for 10 MV FFF (3.85–23.08 Gy/min) it varied from 0.79 to 0.92, for 10 MV 0.72 and for <sup>60</sup>Co  $\gamma$  (0.2 Gy/min) 1.28 at a dose range 0–8 Gy (Fig. 5).

## DISCUSSION

In our study, the spontaneous aberration frequencies appeared to be in agreement with our earlier findings [20]. The yields of dicentric plus rings were 7–20.50/100 cells at 2 Gy irradiation dose, which is in line

**Table 4.** Comparison of linear and quadratic yield coefficients for dicentric aberrations induced by  $^{60}\text{Co}$   $\gamma$  and LINAC X-rays and predicted doses (Gy). Estimated doses (Gy) of the same dicentric (dic + ring) chromosome aberration values based on estimates of parameters for the different calibration curves by CABAS and lower and upper confidence limit (CI, second line in every row) are shown. 95% CI: lower and upper confidence limit. Adapted from data of listed authors and predicted dose was calculated from their dose–response calibration curves with CABAS program: <sup>1</sup>Köksal, 1996; <sup>2</sup>Barquinero, 1995; <sup>3</sup>Wilkins, 2008; <sup>4</sup>Lemos-Pinto, 2015; <sup>5</sup>Vinnikov, 2013; <sup>6</sup>this study.

Irradiation energy, dose rate Gy/min	$\alpha$ -value	$\beta$ -value	Estimated dose, Gy 2 dic + ring/100 cells	Estimated dose, Gy 20 dic + ring/100 cells	Estimated dose, Gy 70 dic + ring/100 cells	Estimated dose, Gy 100 dic + ring/100 cells	Estimated dose, Gy 200 dic + ring/100 cells
$^{60}\text{Co}$ $\gamma^1$ 45.73/Rad/min	0.024	0.069	0.38 0.06–0.85	1.53 1.16–1.94	3.00 2.63–3.40	3.63 3.26–4.02	5.20 4.83–5.58
$^{60}\text{Co}$ $\gamma^2$ 1.07–1.18	0.021 $\pm 0.005$	0.063 $\pm 0.004$	0.39 0.04–0.89	1.59 1.21–2.02	3.12 2.74–3.53	3.77 3.38–4.17	5.39 5.00–5.79
$^{60}\text{Co}$ $\gamma^3$ 0.638	0.029 $\pm 0.008$	0.036 $\pm 0.003$	0.39 0–1.38	1.85 1.24–2.77	3.97 3.25–4.75	4.82 4.10–5.59	
6 MV <sup>4</sup> 0.54	0.013 $\pm 0.007$	0.056 $\pm 0.004$	0.48 0.08–1.02	1.77 <sup>a</sup> 1.36–2.23	3.42 <sup>b</sup> 3.00–3.86	4.11 3.70–4.55	5.87 <sup>n</sup> 5.45–6.30
$^{60}\text{Co}$ $\gamma^5$ 0.5–1.2	0.129 $\pm 0.009$	0.033 $\pm 0.001$	0.14 0.01–0.49	1.17 0.78–1.66	3.02 2.54–3.55	3.86 3.35–4.39	6.02 5.51–6.57
$^{60}\text{Co}$ $\gamma^6$ 0.2	0.005 $\pm 0.018$	0.058 $\pm 0.006$	0.53 0.12–1.06	1.80 1.39–2.25	3.41 3.01–3.85	4.09 3.69–4.52	5.81 5.40–6.23
6 FFF <sup>6</sup> 5.36	0.007 $\pm 0.006$	0.044 $\pm 0.001$	0.58 0.12–1.20	2.06 1.58–2.57	3.93 <sup>c</sup> 3.45–4.42	4.71 <sup>f,h,i</sup> 4.23–5.20	6.70 <sup>n</sup> 6.22–7.18
6 FFF <sup>6</sup> 12.50	0.012 $\pm 0.011$	0.046 $\pm 0.002$	0.77 0.33–1.37	2.21 1.75–2.71	4.03 <sup>b,d</sup> 3.56–4.51	4.78 <sup>g</sup> 4.33–5.26	6.72 <sup>l</sup> 6.26–7.19
6 MV <sup>6</sup> 5.50	0.020 $\pm 0.008$	0.033 $\pm 0.002$	0.51 0.06–1.19	2.16 1.63–2.75	4.28 <sup>d,e</sup> 3.75–4.85	5.18 <sup>h,k</sup> 4.64–5.74	7.44 <sup>m</sup> 6.91–8.00
10 FFF <sup>6</sup> 3.85	0.004 $\pm 0.008$	0.025 $\pm 0.002$	0.84 0.18–1.73	2.90 2.24–3.63	5.51 4.86–6.21	6.61 <sup>f,g,h,k</sup> 5.95–7.30	9.39 <sup>m</sup> 7.39–8.52
10 FFF <sup>6</sup> 15.40	0.013 $\pm 0.011$	0.033 $\pm 0.002$	0.72 0.16–1.45	2.47 1.91–3.08	4.67 4.12–5.26	5.60 <sup>f,h</sup> 5.04–6.18	7.94 <sup>l</sup> 6.77–7.82
10 FFF <sup>6</sup> 23.08	0.007 $\pm 0.012$	0.030 $\pm 0.002$	0.67 0.12–1.41	2.44 1.87–3.06	4.68 4.12–5.28	6.03 <sup>f,g,h,k</sup> 5.44–6.66	8.01 <sup>l</sup> 7.44–8.59
10 MV <sup>6</sup> 5.88	0.0009 $\pm 0.008$	0.023 $\pm 0.002$	0.89 0.23–1.75	2.94 <sup>a</sup> 2.28–3.66	5.52 <sup>c,e</sup> 4.87–6.21	6.61 <sup>i,j</sup> 5.96–7.29	9.36 <sup>m</sup> 8.71–10.03

Differences between estimated doses are significant as indicated: <sup>a</sup> $P = 0.005$ , <sup>b</sup> $P = 0.016$ , <sup>c</sup> $P = 0.0002$ , <sup>d</sup> $P = 0.001$ , <sup>e</sup> $P = 0.005$ , <sup>f</sup> $P = 0.0009$ , <sup>g</sup> $P = 0.005$ , <sup>h</sup> $P = 0.005$ , <sup>i</sup> $P < 0.0001$ , <sup>j</sup> $P = 0.0014$ , <sup>k</sup> $P = 0.043$ , <sup>l</sup> $P = 0.005$ , <sup>m</sup> $P < 0.0001$ , <sup>n</sup> $P = 0.0011$ .

with the values of 12–49/100 cells published by others [24–26]. The dicentric plus ring frequencies were 19–52/100 cells after irradiation with 3 Gy, 80.5–199.7/100 cells at 6 Gy and 104–336/100 cells at 8 Gy. The appearance of these aberrations highly depends on the absorbed dose and energy.

To validate our dose–response curves, the blood samples taken from five more people were irradiated with 3 and 6 Gy. This method is also applicable to get some information about the radiosensitivity of the radiotherapy patients [27]. The frequencies of dicentrics plus rings observed in the individuals—whose blood samples were irradiated with 3 and 6 Gy at 6 MV FFF, 12.5 Gy/min—were counted and dose estimations were done using the proper dose rate curve. Table 5 shows the results of these comparisons. There are some individual differences in the frequencies of dicentric plus ring aberrations found in their lymphocytes, the average difference was 6.3% from the calibration

curve at 3 Gy and 2.7% at 6 Gy. The dose estimation was also done using a  $^{60}\text{Co}$   $\gamma$  (0.2 Gy/min) dose rate curve. The average deviation was 22.3% at 3 Gy and 18.5% at 6 Gy.

We observed significant differences in aberration frequencies when different irradiation techniques were used. The FFF mode has higher radiobiological effect than the FF mode. We have also shown that more dicentric plus ring aberrations were produced by lower energy. Consequently, it seems that the FFF mode does not just have heterogeneous energy spectra, but the effective energy is lower than in the FF mode. This was shown with physical measurements in the publications of Vassiliev *et al.* and Budgell *et al.* [28, 29], but biological measurements are scarce. These phenomena arise because the FF can absorb lower energies better and the depth dose characteristics of the 6 MV FFF beam are similar to those of the 4 MV FF beam. We found that these differences between the FF and FFF radiation techniques

**Table 5.** Cytogenetic effects of LINAC X-ray irradiation in lymphocytes from five individuals' blood samples (before their treatment). Irradiation parameters were: 3 and 6 Gy, 6 FFF mode, 12.5 Gy/min. Dicentric + ring chromosome aberrations (Dic + ring) were counted and the estimated dose was calculated using calibration curves taken either from LINACs (6 FFF mode, 12.5 Gy/min) or from a  $^{60}\text{Co}$  source (0.2 Gy/min) indicated by asterisks (\*). The average deviation from the calibration curve (6 FFF mode, 12.5 Gy/min) was 6.3% at 3 Gy and 2.7% at 6 Gy. These values were 22.3% at 3 Gy and 18.5% at 6 Gy in the case of the  $^{60}\text{Co}$  curve. CI = confidence interval.

No., age, sex	Dic + rings/100 cells		Estimated dose		95% CI interval	
	3Gy	95% CI	3 Gy	6 Gy	3 Gy	6 Gy
1., 75, female	44	143	3.24 2.70*	5.86 4.91*	2.76–3.76 2.29–3.14*	5.37–6.36 4.50–5.33*
2., 72, male	42	156	3.17 2.64*	6.12 5.13*	2.68–3.68 2.23–3.07*	5.64–6.62 4.72–5.55*
3., 64, male	31	120	2.72 2.26*	5.37 4.49*	2.24–3.24 1.85–2.70*	4.88–5.87 4.08–4.91*
4., 63, male	21	127	2.23 1.85*	5.52 4.62*	1.75–2.76 1.44–2.30*	5.04–6.02 4.21–5.04*
5., 76, male	30	168	2.67 2.20*	6.35 5.32*	2.19–3.20 1.81–2.66*	5.87–6.82 4.91–5.73*
Average	33.6	142.8	2.81 2.33*	5.84 4.89*	2.32–3.32 1.92–2.77*	5.36–6.33 4.48–5.31*

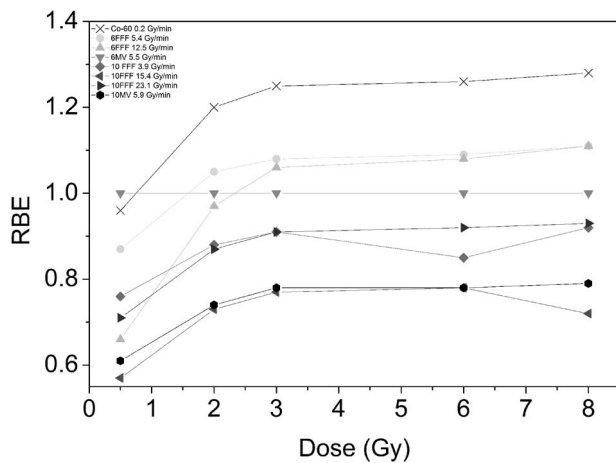


**Fig. 5.** Average RBE values as a function of dose for the photon energies:  $^{60}\text{Co}$   $\gamma$  0.2 Gy/min, 6 FFF (5.4–12.5 Gy/min), 10 MV (5.9 Gy/min) and 10 FFF (3.9–23.1 Gy/min).

(6 MV FF 5.50 Gy/min vs 6 MV FFF 12.5 Gy/min) are most profound in respect of their ability to induce formation of chromosome fragments: 98–128/100 cells vs 228–316/100 cells of dicentrics plus rings at 8 Gy. With regard to calibration curve measurements, we suggest that although for every given technique the standard error increases with the dose, the lower number of aberrations necessitates more evaluated cells in the low dose range. It is also important to measure the effects of different techniques using the same donor's irradiated blood, as individual differences may have an impact on the results.

In our experiments the blood samples were irradiated with photon beams at different dose rates at both 6 and 10 MV FF energy.

While there were differences between the chromosomal aberration frequencies in cells exposed to radiation at different dose rates at the same energy, the change was not always statistically significant. The measurement of Brehwens *et al.* [30] can give some explanation: when dose rate was in the range of  $\sim 10\text{ mGy}-1\text{ Gy/min}$ , DNA repair could take place during the irradiation. Above  $\sim 1\text{ Gy/min}$ , dose was delivered in a much smaller time scale than the time required for lymphocytes to repair DNA, therefore DNA repair could not play a significant role and there was no difference between the effects of dose rates above this level [30]. All of our experiments were done above 1 Gy/min.

We found significant differences in the dose–effect curves of different photon energies, as was expected from previous studies. For example, Hill [31] determined that photons with lower energy are expected to be more effective biologically because they have a higher linear energy transfer value. The energy of secondary electrons emitted is also decreasing, therefore microdosimetric energy depositions show a significant shift in energy deposition patterns towards higher energy. In terms of quantification, cell survival data [30] showed that the RBE value for 200 kV X-rays was  $\sim 10\%$  greater than those for 6 MV photon beams. We determined the RBE of 10 MV compared with 6 MV energies and found a 28% decrease.

In our study, the number of chromatid breaks increased linearly with the dose, however independently of energy or dose rate. Some authors suggested [32, 33] that chromatid-type aberrations were typical for spontaneous chromosomal rearrangements that are probably induced by endogenous reactive oxygen species (ROS). It can be hypothesised, that an increased dose stimulates the production of ROS in mitochondria, and results in a high yield of chromatid-type aberrations, chromatid breaks and exchanges. At low dose irradiation (0–0.5 Gy), the endogenously induced chromatid breaks are commensurable with the ones induced directly by low doses of ionizing radiation [34].

According to our results, at the low dose range (0–2 Gy) the dicentric plus rings represent 13.3–33.3% at 0.5 Gy, 14.3–45.5% at 1.0 Gy and 35–54.9% at 2.0 Gy of the total number of aberrations. In the 3–8 Gy dose range, this value increases to 45–70.2% and depends on energy. Only a few reports contain data on doses at 6 Gy and above [8]. However, in our opinion, the method applied even in these conditions; the only difficulties that we experienced related to scoring excess fragments. Vinnikov and Maznyk [8] investigated higher doses (10, 16 and 20 Gy) and concluded that the main technical complications are related to the poor quality of metaphases and the too high number of chromosomal rearrangements. It seems that other aberrations, which are not radiation specific, are more prominent at low doses. Therefore, the other types of aberrations and total aberration value can also be important indicators of the biological effect of radiation. It would be worth considering using total aberrations instead of dicentric plus rings for biological dosimetry below 2 Gy.

In addition, recent evidence shows that at doses up to 15–18 Gy acentric fragments get into cytosol and can activate an immune response. However, at higher doses the concentration of cytosolic DNA decreases. Finding the correct dose for induction of sufficient double-stranded DNA breaks may be a key step in selecting optimal radiotherapy protocols during immunotherapy [34, 35], and the chromosome aberration method may help to achieve this goal.

To our knowledge, this study is the first comprehensive evaluation of cytogenetic effects of different dose rates in a broad dose range, including very high doses.

### CONCLUSION

The FFF mode increased the biological effect of irradiation. Both dicentric plus rings and  $\beta$  parameters were higher in FFF mode than in FF mode. The calculated order of efficiency is: 6 MV FFF > 6 MV FF > 10 MV FFF > 10 MV FF. The average RBE value for  $^{60}\text{Co}$   $\gamma$  irradiation was 1.28, for 6 MV FFF (5.36–12.5 Gy/min) 1.11, for 10 MV FFF (3.85–23.08 Gy/min) 0.79–0.92 and for 10 MV FF (5.88 Gy/min) 0.72, relative to reference radiation of 6 MV FF with 5.50 Gy/min. These data show that 6 MV FFF has an 11% higher relative biological effect, while the biological damage of 10 MV FF and 10 MV FFF is less than that of 6 MV FF.

In case of accidental overdose of a patient, the appropriate calibration curve should be used. Furthermore, these results can also be useful for selecting the suitable energy and dose rate for clinical practice in the future.

### CONFLICT OF INTEREST

No potential conflict of interest was reported by the authors.

### ACKNOWLEDGMENTS

The technical assistance of Mrs N. Vass and Ms K. Kiss is greatly acknowledged.

### FUNDING

This work was supported by national grant [grant number OTKA K-034416].

### REFERENCES

1. IAEA-International Atomic Energy Agency. Cytogenetic analysis for radiation dose assessment. Technical report series. Vienna 2001.
2. Koksál G, Pala FS, Dalci DO. In vitro dose-response curve for chromosome aberrations induced in human lymphocytes by  $^{60}\text{Co}$  gamma-radiation. *Mutat Res* 1995;3291:57–61.
3. Rungsimaphorn B, Rerkamnuaychoke B, Sudprasert W. Establishment of dose-response curves for Dicentric and premature chromosome condensation for radiological emergency preparedness in Thailand. *Genome Integr* 2016;7:8.
4. Lemos-Pinto MM, Cadena M, Santos N et al. A dose-response curve for biodosimetry from a 6 MV electron linear accelerator. *Braz J Med Biol Res* 2015;4810:908–14.
5. Zubizarreta EH, Poitevin A, Levin CV. Overview of radiotherapy resources in Latin America: A survey by the International Atomic Energy Agency (IAEA). *Radiother Oncol* 2004;731:97–100.
6. Charles M. UNSCEAR report 2000: Sources and effects of ionizing radiation. United Nations scientific Committee on the effects of atomic radiation. *J Radiol Prot* 2001;211:83–6.
7. Xiao Y, Kry SF, Popple R et al. Flattening filter-free accelerators: A report from the AAPM therapy emerging technology assessment work group. *J Appl Clin Med Phys* 2015;163:5219.
8. Vinnikov VA, Maznyk NA. Cytogenetic dose-response in vitro for biological dosimetry after exposure to high doses of gamma-rays. *Radiat Prot Dosimetry* 2013;1542:186–97.
9. Pujol M, Barquinero JF, Puig P et al. A new model of biodosimetry to integrate low and high doses. *PLoS One* 2014;912:e114137.
10. Pujol M, Puig R, Caballin MR et al. The use of caffeine to assess high dose exposures to ionising radiation by dicentric analysis. *Radiat Prot Dosimetry* 2012;1494:392–8.
11. Ling CC, Gerweck LE, Zaider M et al. Dose-rate effects in external beam radiotherapy redux. *Radiother Oncol* 2010;953:261–8.
12. Lohse I, Lang S, Hrbacek J et al. Effect of high dose per pulse flattening filter-free beams on cancer cell survival. *Radiother Oncol* 2011;1011:226–32.
13. Verbakel WF, van den Berg J, Slotman BJ et al. Comparable cell survival between high dose rate flattening filter free and conventional dose rate irradiation. *Acta Oncol* 2013;523:652–7.
14. Stankeova S, Crompton NE, Blattmann H et al. Apoptotic response of irradiated T-lymphocytes. An epidemiologic study in canine radiotherapy patients. *Strahlenther Onkol* 2003;17911:779–86.
15. Garcia-Sagredo JM. Fifty years of cytogenetics: A parallel view of the evolution of cytogenetics and genotoxicology. *Biochim Biophys Acta* 2008;17796-7:363–75.
16. Carrano AV, Natarajan AT. International Commission for Protection against Environmental Mutagens and Carcinogens. ICPEMC publication no. 14. Considerations for population monitoring using cytogenetic techniques. *Mutat Res* 1988;2043:379–406.
17. Merkle W. Poisson goodness-of-fit tests for radiation-induced chromosome aberrations. *Int J Radiat Biol Relat Stud Phys Chem Med* 1981;406:685–92.



18. Deperas J, Szluinska M, Deperas-Kaminska M et al. CABAS: A freely available PC program for fitting calibration curves in chromosome aberration dosimetry. *Radiat Prot Dosimetry* 2007;1242:115–23.
19. Barillot C, Benali H, Dojat M et al. Federating distributed and heterogeneous information sources in neuroimaging: The NeuroBase project. *Stud Health Technol Inform* 2006;120:3–13.
20. Farkas G, Juranyi Z, Szekely G et al. Relationship between spontaneous frequency of aneuploidy and cancer risk in 2145 healthy Hungarian subjects. *Mutagenesis* 2016;31:583–588.
21. Wilkins RC, Romm H, Kao TC et al. Interlaboratory comparison of the dicentric chromosome assay for radiation biodosimetry in mass casualty events. *Radiat Res* 2008;169S:551–60.
22. Prasanna PG, Moroni M, Pellmar TC. Triage dose assessment for partial-body exposure: Dicentric analysis. *Health Phys* 2010;982:244–51.
23. Barquinero JF, Barrios L, Caballin MR et al. Establishment and validation of a dose-effect curve for gamma-rays by cytogenetic analysis. *Mutat Res* 1995;3261:65–9.
24. Sasaki MS. Chromosomal biodosimetry by unfolding a mixed Poisson distribution: A generalized model. *Int J Radiat Biol* 2003;792:83–97.
25. Yao B, Jiang BR, Ai HS et al. Biological dose estimation for two severely exposed patients in a radiation accident in Shandong Jining, China, in 2004. *Int J Radiat Biol* 2010;869:800–8.
26. Chen Y, Yan XK, Du J et al. Biological dose estimation for accidental supra-high dose gamma-ray exposure. *Radiation Measurements* 2011;469:837–41.
27. Borgmann K, Hoeller U, Nowack S et al. Individual radiosensitivity measured with lymphocytes may predict the risk of acute reaction after radiotherapy. *Int J Radiat Oncol Biol Phys* 2008;711:256–64.
28. Vassiliev ON, Titt U, Ponisch F et al. Dosimetric properties of photon beams from a flattening filter free clinical accelerator. *Phys Med Biol* 2006;517:1907–17.
29. Budgell G, Brown K, Cashmore J et al. IPEM topical report 1: Guidance on implementing flattening filter free (FFF) radiotherapy. *Phys Med Biol* 2016;6123:8360–94.
30. Brehwens K, Staaf E, Haghdoost S et al. Cytogenetic damage in cells exposed to ionizing radiation under conditions of a changing dose rate. *Radiat Res* 2010;1733:283–9.
31. Hill MA. The variation in biological effectiveness of X-rays and gamma rays with energy. *Radiat Prot Dosimetry* 2004;1124:471–81.
32. Pollycove M, Feinendegen LE. Radiation-induced versus endogenous DNA damage: Possible effect of inducible protective responses in mitigating endogenous damage. *Hum Exp Toxicol* 2003;226:290–306 discussion 307, 315-7, 319-23.
33. Kryston TB, Georgiev AB, Pissis P et al. Role of oxidative stress and DNA damage in human carcinogenesis. *Mutat Res* 2011;7111-2:193–201.
34. Durante M, Formenti SC. Radiation-induced chromosomal aberrations and immunotherapy: Micronuclei, cytosolic DNA, and interferon-production pathway. *Front Oncol* 2018;8:192.
35. Vanpouille-Box C, Formenti SC, Demaria S. Toward precision radiotherapy for use with immune checkpoint blockers. *Clin Cancer Res* 2018;242:259–65.